Chemical Physics 501 (2018) 1–7

Contents lists available at ScienceDirect

Chemical Physics

journal homepage: www.elsevier.com/locate/chemphys

On the solvation of hydronium by carbon dioxide: Structural and infrared spectroscopic study of $(H_3O^+)(CO_2)_n$

Jianpeng Yang [a,*], Xiangtao Kong [b], Ling Jiang [b,*]

[a] College of Chemistry and Chemical Engineering, Xinyang Normal University, Xinyang 464000, China
[b] State Key Laboratory of Molecular Reaction Dynamics, Collaborative Innovation Center of Chemistry for Energy and Materials, Dalian Institute of Chemical Physics, Chinese Academy of Sciences, 457 Zhongshan Road, Dalian 116023, China

ARTICLE INFO

Article history:
Received 2 September 2017
In final form 21 November 2017
Available online 22 November 2017

Keywords:
Hydronium
Carbon dioxide
Solvation
Infrared photodissociation spectroscopy
Quantum chemical calculation

ABSTRACT

Hydronium (H_3O^+) is the smallest member of protonated water. In this work, we use quantum chemical calculations to explore the solvation of H_3O^+ by adding one CO_2 molecule at a time. The effect of stepwise solvation on infrared spectroscopy, structure, and energetics has been systematically studied. It has been found that the first solvation shell of H_3O^+ is completed at $n = 6$. Besides the hydrogen-bond interaction, the C_{CO2}—O_{CO2} intermolecular interaction is also responsible for the stabilization of the larger clusters. The transfer of the proton from H_3O^+ onto CO_2 with the formation of the $OCOH^+$ moiety is not observed in the early stage of solvation process. Calculated IR spectra suggest that vibrational frequencies of H-bonded O—H stretching would afford a sensitive probe for exploring the early stage solvation of hydronium by carbon dioxide. IR spectra for the $(H_3O^+)(CO_2)_n$ ($n = 1–7$) clusters could be measured by the infrared photodissociation spectroscopic technique and thus provide a vivid physical picture about how carbon dioxide solvates the hydronium.

1. Introduction

Hydronium (H_3O^+) is the cation that forms from water in the presence of hydrogen ions. Hydronium is also an abundant molecular ion in the interstellar medium and is found in diffuse and dense molecular clouds as well as the plasma tails of comets [1]. The solvation of hydronium ion in water has been extensively investigated because of its fundamental importance in biological, atmospheric, and interstellar chemistry. Numerous excellent reviews addressing these aspects are available in the literature summarizing the experimental and theoretical studies on the spectroscopy, structure, and dynamics of water; see, for example, Refs. [2–9]. Microhydration studies provide detailed energetic and structural information that is difficult to extract from measurement of bulk solutions. The $H^+(H_2O)_6$ system is the smallest protonated water cluster for which both Eigen-type ($H_3O^+(H_2O)_3$) and Zundel-type (H_2O-H^+-OH_2) characteristic binding motifs coexist [10–12]. Infrared (IR) spectroscopy of $H^+(H_2O)_n$ has revealed that the chain structures at small sizes ($n \leq 10$) develop into two dimensional net structures ($\sim 10 < n < 21$), and then into nanometer-scaled cages ($n \geq 21$) [13]. Ab initio molecular dynamics (AIMD) simulations have shown that the umbrella inversion mode can either trap or release the proton from different parts of the water network [14]. AIMD study on the propensity of the excess proton for the air-water interface has indicated that the enhanced water structuring around the proton results in the presence of proton wires that run parallel to the surface as well as a hydrophobic environment [15]. Interestingly, protons in liquid water are found to be primarily hydrated by two flanking water molecules, with a broad range of proton hydrogen bond lengths and asymmetries [16].

The solvation of the hydroxide (OH^-) has also been the subject of many experimental and theoretical studies in the range from clusters to bulk [9,17–20]. Recently, theoretical investigation of the $OH^-(H_2O)_{20}$ cluster has revealed that the OH^- has an amphiphilic Janus-type behavior like the hydronium ion induced by the ability of its O—H bond to be buried inside of the cluster or exposed at the surface with different coordination numbers [19]. It has been demonstrated that the IR spectrum of the bare hydroxide ion as well as the water molecule donating a hydrogen bond to it exhibits characteristic absorption along the amphiphilic band between 1500 and 3000 cm^{-1} at positions very similar to those found for the entire hydroxide cluster [20].

Both theoretical and experimental investigations on the CO_2 clusters have also received substantial attention during the last

* Corresponding authors.
E-mail addresses: yangjpchem@126.com (J. Yang), ljiang@dicp.ac.cn (L. Jiang).

https://doi.org/10.1016/j.chemphys.2017.11.015
0301-0104/

two decades, in that CO_2 is a double-faceted gas as an abundant renewable resource for the production of fine chemicals and clean fuels and a main contributor to global warming [21–26]. Recently, the structure and the energetics of H_2O-CO_2 binary systems have been explored experimentally and theoretically [21,22,25,27–30]. For instance, infrared photodissociation (IRPD) spectroscopy of the anionic $[(H_2O)_m(CO_2)_n]^-$ (m = 1, 2; n = 1–4) clusters indicates that the formation of target clusters possibly involves the $(H_2O)_m(CO_2)_n + e^-$ collisions followed by electron capture, ion-core formation, solvent migration, and evaporative cooling [28]. For the cationic clusters, time of flight (TOF) mass spectroscopy of H_2O-CO_2 binary clusters with single photon ionization at 26.5 eV has indicated that the formation of the protonated $H^+(H_2O)_n(CO_2)$ clusters is favored at low CO_2 concentration (i.e., 5% CO_2 partial pressures), whereas the formation of the unprotonated $[(H_2O)_{1,2}(CO_2)_n]^+$ clusters is preferred at high CO_2 concentration (i.e., 20% CO_2 partial pressures) [21]. IRPD spectra of the unprotonated $[(H_2O)(CO_2)_n]^+$ clusters show that the first two CO_2 molecules bind to the OH groups of the H_3O^+ ion core and the third and the fourth CO_2 molecules are solvated to the oxygen atom of the H_3O^+ ion core from out of the plane of H_3O^+, completing the first solvation shell at n = 4 [30]. Recently, quantum chemical calculations of neutral $[(H_2O)_m(CO_2)_n]$ (m = 1–3; n = 1–12) clusters indicated that seven CO_2 molecules form the first solvent shell of a single H_2O with four CO_2 molecules interacting with the H_2O via Lewis acid-base interactions, two CO_2 interacting with the H_2O by hydrogen bonds, and the seventh CO_2 completing the shell [25]. Ab initio molecular dynamics (AIMD) study of the recombination mechanism of the proton with the CO_3^{2-} ion revealed that the proton transfer is mediated by the water wires [31].

So far, much less efforts have been made for the study on the interaction of protonated water with a number of carbon dioxide. Herein, we report a theoretical investigation of the solvation of hydronium by carbon dioxide via a cluster model. The hydronium ion was chosen in this work because it represents the smallest member of protonated water. The effect of stepwise solvation on infrared spectroscopy, structure, and energetics was systematically explored. It has been found that the first solvation shell of hydronium is completed at n = 6. Calculated IR spectra reveal that vibrational frequencies of H-bonded O—H stretching afford a sensitive probe for exploring the early stage solvation of hydronium by carbon dioxide.

2. Theoretical methods

Quantum chemical calculations were performed using Gaussian 09 program suite [32]. Initial configurations were built on the basis of the relevant structures reported in the literature. Previous studies indicated that the interaction of water and/or methanol with carbon dioxide could be properly predicted by the M06-2X functional [7,11,26,33], which was also employed for the present calculations. The 6-311++G(d,p) basis set was used for the H, C, and O atoms. Tight convergence of the optimization and the self-consistent field procedures was imposed, and an ultrafine grid was used. Relative and dissociation energies included the zero-point-energy corrections. Harmonic vibrational frequencies were calculated at the same level. All reported structures were true minima without imaginary vibrational frequencies. Simulated IR spectra were derived from M06-2X/6-311++G(d,p) harmonic vibrational frequencies and intensities. Harmonic vibrational frequencies are scaled by a factor of 0.966, which was determined by the comparison of simulated vibrational frequencies of O—C—O stretching for CO_2 unit in the $(H_3O^+)(CO_2)_2$ cluster with the experimental value [30]. IR stick spectra were convoluted by a Gaussian line shape function with a width of 10 cm^{-1} (fwhm).

3. Results and discussion

3.1. Solvation motifs and IR spectra

Fig. 1 shows the representative low-lying structures of the $(H_3O^+)(CO_2)_n$ (n = 1–7) clusters. The structures are labeled according to the number of CO_2 molecules and relative energies. Figs. 2–6 show the calculated IR spectra of the representative low-lying isomers in the spectra range of 800–3800 cm^{-1}. Harmonic vibrational frequencies and intensities of the free O—H stretching, H-bonded O—H stretching, and O—C—O stretching of CO_2 unit for the lowest-lying isomers of $(H_3O^+)(CO_2)_n$ (n = 1–7) are listed in Table 1.

3.1.1. n = 1

In Fig. 1, the structure of $(H_3O^+)(CO_2)$ (labeled 1A) has an ion-molecule form, $H_3O^+ \cdots CO_2$, which is reasonable because the proton affinity of H_2O (691.0 kJ/mol) is higher than that of CO_2 (540.5 kJ/mol) [34]. CO_2 forms one H-bond (1.51 Å) with one OH group, leaving another two OH groups free. The calculated IR spectrum of 1A (Fig. 2, trace 1A) shows three main absorption features. Two weak peaks at 3596 and 3667 cm^{-1} (labeled free ν_{OH}) are 61 and 89 cm^{-1} red-shifted from the symmetric (3657 cm^{-1}) and antisymmetric (3756 cm^{-1}) stretching vibrational frequencies of the free water molecule, respectively, reflecting the softening of these modes upon complexation as bonding electron density is withdrawn from the water molecule [35,36]. The intense peak at 2779 cm^{-1} is due to the H-bonded O—H stretching vibrations (labeled H-bonded ν_{OH}). The peak at 2418 cm^{-1} corresponds to the O—C—O stretching vibration for CO_2 unit (labeled ν_{OCO}).

3.1.2. n = 2

Addition of a second CO_2 molecule yields the C_s structure, labeled 2A, in which the two CO_2 molecules are symmetry-equivalent and both form a strong H-bond (1.61 Å) to one of the

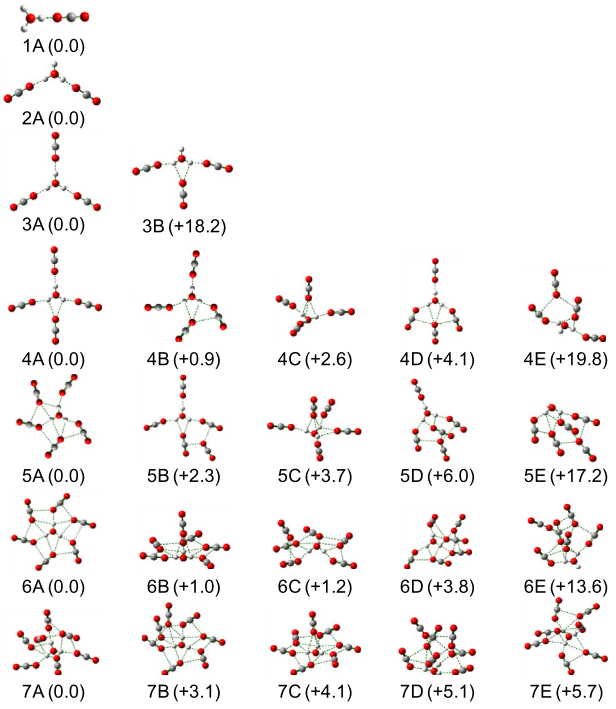

Fig. 1. Optimized structures of the $(H_3O^+)(CO_2)_n$ (n = 1–7) clusters (C, gray; H, light gray; O, red). Relative energies are given in kJ/mol. (For interpretation of the references to colour in this figure legend, the reader is referred to the web version of this article.)

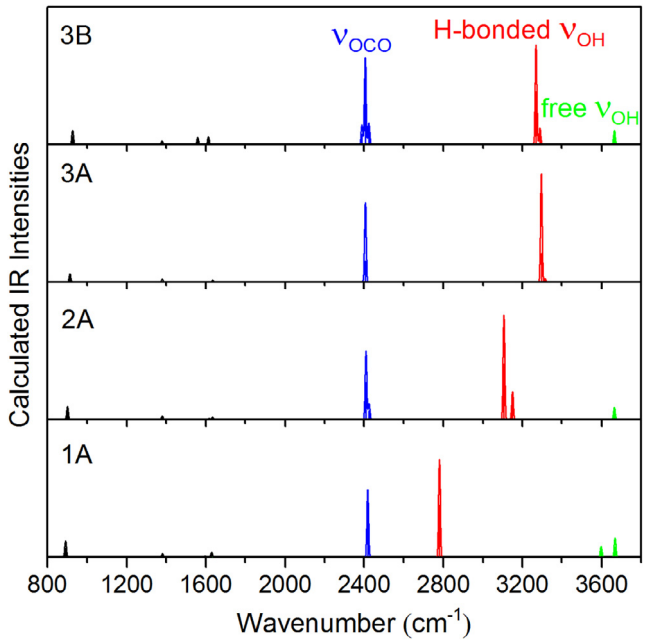

Fig. 2. Simulated IR spectra of the three optimized isomers of $(H_3O^+)(CO_2)_n$ (n = 1–3). Assignments of free O—H stretching, H-bonded O—H stretching, and O—C—O stretching for CO_2 unit are indicated in green, red, and blue, respectively. (For interpretation of the references to colour in this figure legend, the reader is referred to the web version of this article.)

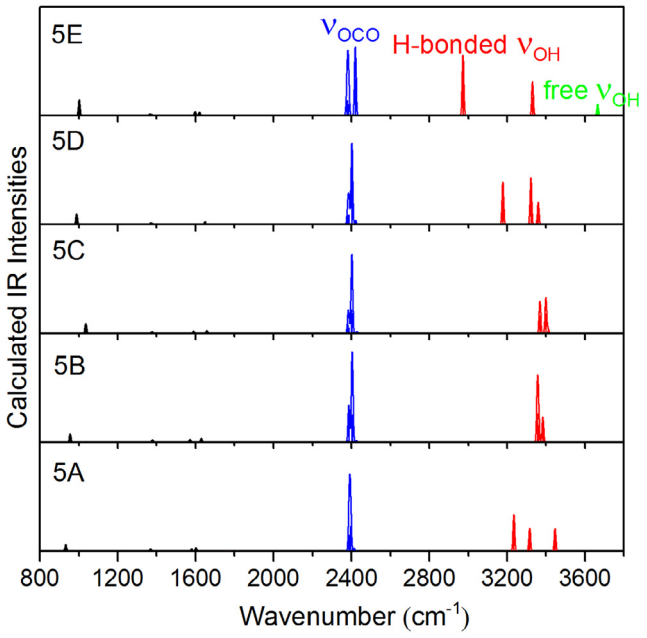

Fig. 4. Simulated IR spectra of the three optimized isomers of $(H_3O^+)(CO_2)_5$. Assignments of free O—H stretching, H-bonded O—H stretching, and O—C—O stretching for CO_2 unit are indicated in green, red, and blue, respectively. (For interpretation of the references to colour in this figure legend, the reader is referred to the web version of this article.)

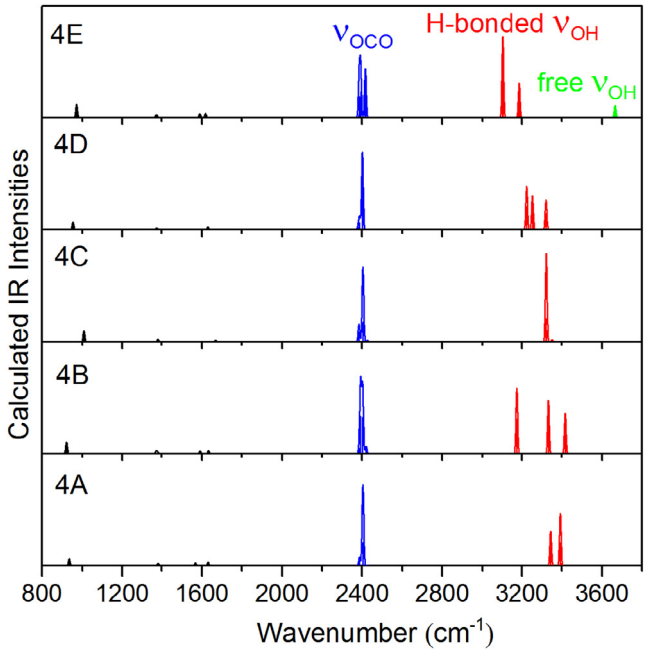

Fig. 3. Simulated IR spectra of the three optimized isomers of $(H_3O^+)(CO_2)_4$. Assignments of free O—H stretching, H-bonded O—H stretching, and O—C—O stretching for CO_2 unit are indicated in green, red, and blue, respectively. (For interpretation of the references to colour in this figure legend, the reader is referred to the web version of this article.)

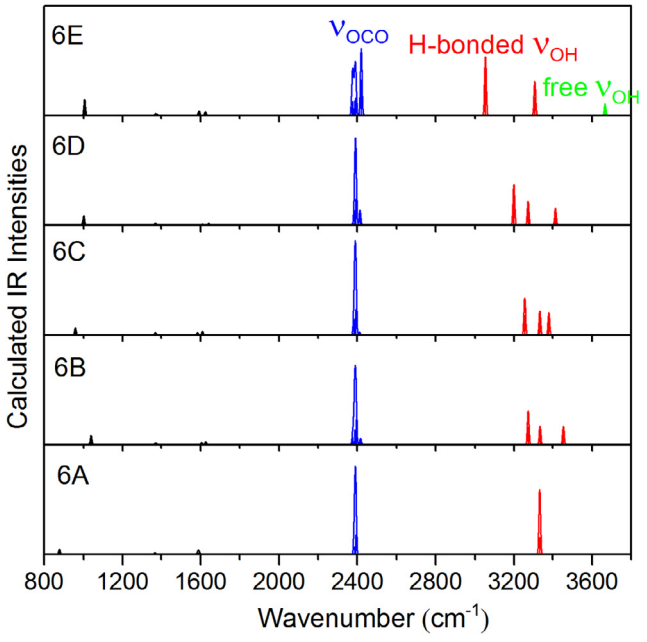

Fig. 5. Simulated IR spectra of the three optimized isomers of $(H_3O^+)(CO_2)_6$. Assignments of free O—H stretching, H-bonded O—H stretching, and O—C—O stretching for CO_2 unit are indicated in green, red, and blue, respectively. (For interpretation of the references to colour in this figure legend, the reader is referred to the web version of this article.)

hydronium H-atoms (Fig. 1). In the simulated IR spectrum of 2A (Fig. 2, trace 2A), the free ν_{OH} mode is calculated to be 3663 cm^{-1} (Table 1). The peaks at 3106 and 3150 cm^{-1} are due to the H-bonded ν_{OH} mode, which probably converge to one band in the experimental spectrum. The band centered around 2400 cm^{-1} is responsible for the ν_{OCO} mode.

3.1.3. n = 3

The lowest energy isomer for the n = 3 cluster, 3A, is a C_{3v} structure, in which the CO_2 molecules form three H-bonds (1.67 Å) with H_3O^+ (Fig. 1). The 3B isomer lies 18.2 kJ/mol higher in energy than 3A and consists of four H-bonds, leaving one free OH group. It can be found that the most stable structure of protonated $(H_3O^+)(CO_2)_3$ cluster is different from that of unprotonated $(H_2O^+)(CO_2)_3$ cluster

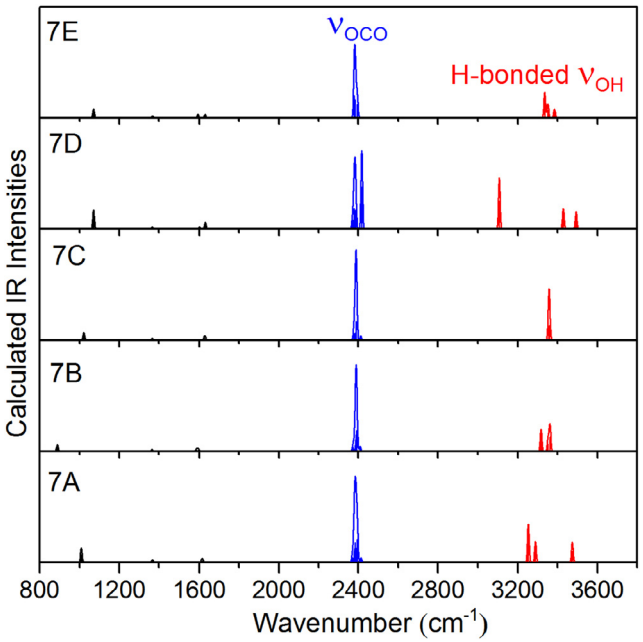

Fig. 6. Simulated IR spectra of the three optimized isomers of $(H_3O^+)(CO_2)_7$. Assignments of free O—H stretching, H-bonded O—H stretching, and O—C—O stretching for CO_2 unit are indicated in green, red, and blue, respectively. (For interpretation of the references to colour in this figure legend, the reader is referred to the web version of this article.)

in which two CO_2 molecules are bound to the OH groups in the plane, and the other one is located out of the plane of the ion core [30]. The simulated IR spectrum of 3A (Fig. 2, trace 3A) includes two intense peaks at 2406 and 3296 cm^{-1}, which correspond to the ν_{OCO} and H-bonded ν_{OH} modes, respectively. In the simulated IR spectrum of 3B (Fig. 2, trace 3B), the ν_{OCO}, H-bonded ν_{OH}, and free ν_{OH} modes are observed at 2406, 3269, and 3664 cm^{-1}, respectively. In 3A, all the OH groups are solvated by three CO_2, resulting in the absence of the free ν_{OH} mode, which is quite different from 3B. Since the free O—H stretching has been readily resolved in the IRPD spectra of a series of mass-selected clusters [6,28,30,37–40], the existence of 3B could be confirmed by the experimental IRPD measurement.

3.1.4. n = 4

In the lowest energy isomer for the $n = 4$ cluster, 4A, the first three CO_2 molecules form three H-bonds with H_3O^+ and the fourth CO_2 forms two H-bonds with H_3O^+, as shown in Fig. 1. In the 4B structure, the fourth CO_2 forms two H-bonds with H_3O^+ and one C_{CO2}—O_{CO2} intermolecular interaction, which lies only 0.9 kJ/mol higher in energy than 4A. The 4C isomer (+2.6 kJ/mol) could be viewed as the derivative of 3A, in which the fourth CO_2 vertically attaches onto the top of the plane of the H_3O^+ ion core. In the 4D isomer (+4.1 kJ/mol), the fourth CO_2 forms two H-bonds with H_3O^+ and two C_{CO2}—O_{CO2} intermolecular interactions. The 4E isomer consists of one free OH group, which is located above 4A by 19.8 kJ/mol. In the simulated IR spectra of 4A–4E (Fig. 3), the H-bonded ν_{OH} mode is observed with remarkably different splittings. The free ν_{OH} mode appears only in the 4E isomer.

3.1.5. n = 5

The lowest energy isomer for the $n = 5$ cluster, 5A, could be viewed as the derivative of 4B, in which the fifth CO_2 forms two H-bonds with H_3O^+ and one C_{CO2}—O_{CO2} intermolecular interaction, as shown in Fig. 1. The 5B isomer could be viewed as the

Table 1
Simulated vibrational frequencies (cm^{-1}) and intensities (km/mol, in parenthesis) of free O—H stretching, H-bonded O—H stretching, and O—C—O stretching of CO_2 unit for the lowest-lying isomers of $(H_3O^+)(CO_2)_n$ ($n = 1$–7) together with the lowest dissociation energies for the loss of one CO_2 molecule (E_{diss}, kJ/mol), CO_2-sovlated O—H bond lengths (R_{O-H}, Å) and Wiberg bond order of the OH moiety (P_{O-H}).

Species	Free ν_{OH}	H-bonded ν_{OH}	ν_{OCO}	E_{diss}	R_{O-H}	P_{O-H}
1A	3667 (447) 3596 (253)	2779 (2268)	2418 (1569)	63.69	1.018	0.56
2A	3663 (357)	3150 (820) 3106 (3071)	2425 (481) 2409 (2024)	49.71	0.998	0.60
3A		3315 (140) 3296 (2439) 3296 (2440)	2425 (20) 2406 (1786) 2406 (1786)	42.70	0.989	0.62
4A		3392 (464) 3391 (2027) 3343 (1637)	2426 (35) 2405 (1849) 2403 (2081) 2387 (424)	22.43	0.988 0.986	0.63 0.62
5A		3446 (1111) 3316 (1115) 3234 (1786)	2412 (148) 2394 (2262) 2389 (1325) 2387 (1491) 2386 (3)	22.43	0.993 0.989 0.983	0.61 0.62 0.63
6A		3333 (1855) 3332 (1867) 3329 (96)	2407 (7) 2391 (2319) 2391 (2133) 2385 (856) 2385 (859) 2385 (37)	20.61	0.989	0.62
7A		3437 (816) 3288 (831) 3252 (1546)	2413 (200) 2394 (1717) 2387 (1079) 2385 (1502) 2381 (1058) 2379 (878) 2371 (368)	22.54	0.993 0.992 0.983	0.61 0.61 0.64

derivative of 4A, in which the fifth CO_2 forms two C_{CO2}—O_{CO2} intermolecular interactions, which lies 2.3 kJ/mol higher in energy than 5A. The structures of 5C–5E are similar to those of 4C–4E. Fig. 4 shows the simulated IR spectra of 5A–5E. The H-bonded ν_{OH} and ν_{OCO} modes are observed in all the isomers, whereas the free ν_{OH} mode appears only in the 5E isomer.

3.1.6. n = 6 and 7

The lowest energy isomer for the $n = 6$ cluster, 6A, is a C_3 structure and could be viewed as the derivative of 5A, in which the sixth CO_2 forms two H-bonds with H_3O^+ and one C_{CO2}—O_{CO2} intermolecular interaction, as shown in Fig. 1. The structures of 6B–6E consist of CO_2 in the second solvation shell. The simulated IR spectra of 6A–6E are depicted in Fig. 5. The H-bonded ν_{OH} mode sharply presents in the simulated IR spectra of 6A. Remarkable splittings for the H-bonded ν_{OH} mode appear in the simulated IR spectra of 6B-6E. The free ν_{OH} mode is only observed in the simulated IR spectra of 6E.

In the 7A–7C structures, the additional CO_2 molecules extend the H_3O-CO_2 and CO_2-CO_2 network and form a second solvation layer. In the simulated IR spectra of 7A–7F (Fig. 6), the H-bonded ν_{OH} mode is remarkably observed. The free ν_{OH} mode is absent in all the isomers of $n = 7$.

3.2. General trend

Fig. 7 shows the comparison of the calculated IR spectra of the lowest-lying isomers for the $(H_3O^+)(CO_2)_n$ ($n = 1–7$) clusters. The lowest dissociation energies for the loss of one CO_2 molecule, CO_2-sovlated O—H bond lengths, and Wiberg bond order of the OH moiety are summarized in Table 1.

It can be seen from the aforementioned solvation motifs that the CO_2 molecules prefer to bind to the OH groups of hydronium. A maximum of three CO_2 molecules interact directly with hydronium. Besides the H-bond interaction, the additional CO_2 molecules starts to form the C_{CO2}—O_{CO2} intermolecular interaction in the larger clusters, completing the first coordination shell at $n = 6$. The transfer of the proton from hydronium onto CO_2 with the formation of the $OCOH^+$ moiety is not observed in the early stage of solvation process. Previous IRPD spectroscopic studies of $(H_2O^+)(CO_2)_n$ ($n = 1–7$) suggest that the first two CO_2 molecules are hydrogen bonded to both of the OH groups of the H_2O^+ ion core, and the third and the fourth CO_2 molecules are bound to the oxygen atom of the H_2O^+ ion core, filling the first solvation shell of the H_2O^+ ion core at $n = 4$ [30]. Analogously, the first CO_2 molecule is bonded to the OH group of the unprotonated methanol (CH_3OH^+) ion core and the second and third CO_2 molecules are bonded to the oxygen atom of the CH_3OH^+ ion core [30]. Recent theoretical investigations of the protonated $H^+(CH_3OH)(CO_2)_n$ ($n = 1–7$) clusters indicate that the first solvation shell of the OH groups is completed at $n = 3$ or 4 [33].

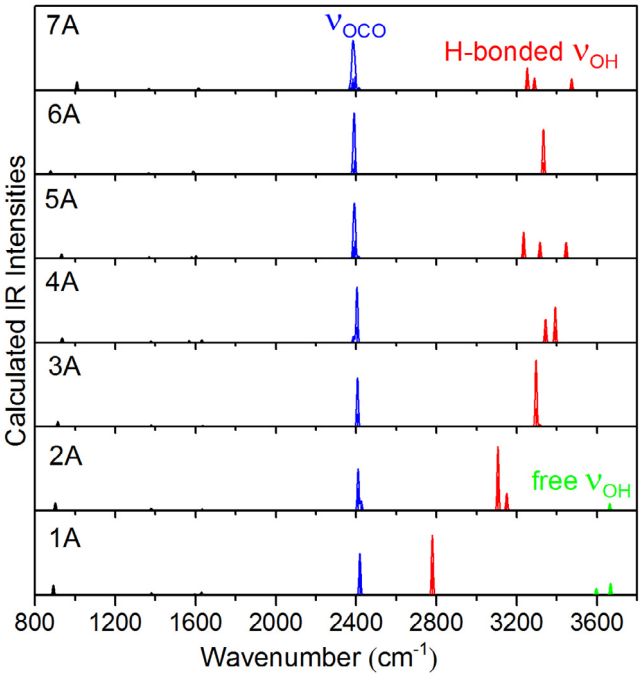

Fig. 7. Simulated IR spectra of the lowest-lying isomers of $(H_3O^+)(CO_2)_n$ ($n = 1–7$). Assignments of free O—H stretching, H-bonded O—H stretching, and O—C—O stretching for CO_2 unit are indicated in green, red, and blue, respectively.

As illustrated in Fig. 7, the $n = 1–2$ cluster exhibits three groups of absorptions for free ν_{OH}, H-bonded ν_{OH}, and ν_{OCO}, while the $n = 3–7$ clusters feature two modes of H-bonded ν_{OH} and ν_{OCO}. The vibrational frequency of the H-bonded ν_{OH} mode is blue-shifted with the increase of cluster size and shows slight change around $n = 6$, indicating that the solvation of the OH groups of hydronium approaches to be converged around $n = 6$. The lowest dissociation energy for the loss of one CO_2 molecule for nA ($n = 1–7$) is 63.69, 49.71, 42.70, 22.43, 22.43, 20.61, and 22.54 kJ/mol, respectively (Table 1), supporting the above-mentioned trend of the solvation. Similar evidence could be obtained from CO_2-sovlated O—H bond lengths and Wiberg bond order (Table 1).

IRPD spectroscopy has emerged as a powerful tool for the structural characterization of mass-selected clusters [6,38,41–45]. Under readily achievable experimental conditions, absorption of single IR photon or multiple IR photons by a cluster can induce a measurable increase in the sequence, resulting in IRPD spectra that closely resemble linear absorption spectra. In contrast with the conventional Fourier Transform infrared spectroscopy, IRPD spectroscopy has advantages of high selectivity and high sensitivity. Considering that free O—H stretching, H-bonded O—H stretching, and O—C—O stretching of CO_2 unit have been successfully resolved in the IRPD spectra of a series of mass-selected clusters radiated by optical parametric oscillator/optical parametric amplifier (OPO/OPA) table-top laser system or infrared free electron laser (IR-FEL) source [6,28,30,37–40], the predicted IR spectra for the $(H_3O^+)(CO_2)_n$ ($n = 1–7$) clusters could be readily measured by the IRPD technique and thus afford useful information for the understanding of early stage solvation of protonated water by carbon dioxide.

Note that the isomerization barrier in-between the 4A and 4B structures for $(H_3O^+)(CO_2)_4$ was calculated to be 0.4 kJ/mol at the M06-2X/6-311++G(d,p) level of theory. The configuration transformation of such weakly bonded molecular clusters might occur because of flat potential energy surface. For instance, IRPD spectroscopic and theoretical studies of mass-selected $H^+(H_2O)_6$ cluster reveal the coexistence of multiple isomers [11,12]. For some hydrated clusters, both quantum chemical calculations and molecular dynamics simulations are needed to interpret the experimental IR spectra [9,46–48]. AIMD simulation makes use of quantum mechanics for the electronic structure, which is a valuable tool in unraveling the molecular origins underlying the spectra [49]. Nuclear quantum effects have been shown to significantly enhance the delocalization of protons in various hydrogen-bonded systems [9]. A first-principles quantum mechanical treatment of both the electrons and nuclei can be achieved by the use of ab initio path integral molecular dynamics (PIMD) simulations [50]. A step closer to agreement between experiment and theory for a given system could be converged by the application of high-level quantum chemical methods, PIMD simulations, and the related methods [50–53].

4. Conclusion

The effect of solvation on the conformation of the smallest protonated water, H_3O^+, has been studied by adding one CO_2 molecule at a time. Quantum chemical calculations of the $(H_3O^+)(CO_2)_n$ (n = 1–7) clusters indicate that the first solvation shell of H_3O^+ is completed at n = 6. Besides hydrogen-bond interaction, the C_{CO2}—O_{CO2} intermolecular interaction is also responsible for the stabilization of the larger clusters. The transfer of the proton from H_3O^+ onto CO_2 with the formation of the $OCOH^+$ moiety might be unfavorable in the early stage of solvation process. Calculated IR spectra reveal that vibrational frequencies of H-bonded O—H stretching would afford a sensitive probe for exploring the early stage solvation of hydronium by carbon dioxide. The combination of IRPD technique and theoretical modeling thus provide useful information for the understanding of solvation processes of hydronium by carbon dioxide.

Acknowledgements

This work was supported by the National Natural Science Foundation of China (Grant Nos. 21327901 and 21673231), the Key Research Programme (Grant No. KGZD-EW-T05), and the Strategic Priority Research Programme (Grant No. XDB17010000) of the Chinese Academy of Science.

References

[1] J.M. Hollis, E.B. Churchwell, E. Herbst, F.C. Delucia, An interstellar line coincident with the p(2,1) transition of hydronium (H_3O^+), Nature 322 (1986) 524–526.
[2] F.N. Keutsch, J.D. Cruzan, R.J. Saykally, The water trimer, Chem. Rev. 103 (2003) 2533–2577.
[3] H.C. Chang, C.C. Wu, J.L. Kuo, Recent advances in understanding the structures of medium-sized protonated water clusters, Int. Rev. Phys. Chem. 24 (2005) 553–578.
[4] D. Marx, A. Chandra, M.E. Tuckerman, Aqueous basic solutions: Hydroxide solvation, structural diffusion, and comparison to the hydrated proton, Chem. Rev. 110 (2010) 2174–2216.
[5] C. Knight, G.A. Voth, The curious case of the hydrated proton, Acc. Chem. Res. 45 (2012) 101–109.
[6] A. Fujii, K. Mizuse, Infrared spectroscopic studies on hydrogen-bonded water networks in gas phase clusters, Int. Rev. Phys. Chem. 32 (2013) 266–307.
[7] S.R. Gadre, S.D. Yeole, N. Sahu, Quantum chemical investigations on molecular clusters, Chem. Rev. 114 (2014) 12132–12173.
[8] N. Heine, K.R. Asmis, Cryogenic ion trap vibrational spectroscopy of hydrogen-bonded clusters relevant to atmospheric chemistry, Int. Rev. Phys. Chem. 34 (2015) 1–34.
[9] N. Agmon, H.J. Bakker, R.K. Campen, R.H. Henchman, P. Pohl, S. Roke, M. Thaemer, A. Hassanali, Protons and hydroxide ions in aqueous systems, Chem. Rev. 116 (2016) 7642–7672.
[10] J.C. Jiang, Y.S. Wang, H.C. Chang, S.H. Lin, Y.T. Lee, G. Niedner-Schatteburg, H.C. Chang, Infrared spectra of $H^+(H_2O)_{5-8}$ clusters: Evidence for symmetric proton hydration, J. Am. Chem. Soc. 122 (2000) 1398–1410.
[11] K. Mizuse, A. Fujii, Infrared photodissociation spectroscopy of $H^+(H_2O)_6$-M (M = Ne, Ar, Kr, Xe, H_2, N_2, and CH_4): messenger-dependent balance between H_3O^+ and $H_5O_2^+$ core isomers, Phys. Chem. Chem. Phys. 13 (2011) 7129–7135.
[12] N. Heine, M.R. Fagiani, M. Rossi, T. Wende, G. Berden, V. Blum, K.R. Asmis, Isomer-selective detection of hydrogen-bond vibrations in the protonated water hexamer, J. Am. Chem. Soc. 135 (2013) 8266–8273.
[13] M. Miyazaki, A. Fujii, T. Ebata, N. Mikami, Infrared spectroscopic evidence for protonated water clusters forming nanoscale cages, Science 304 (2004) 1134–1137.
[14] A.A. Hassanali, F. Giberti, G.C. Sosso, M. Parrinello, The role of the umbrella inversion mode in proton diffusion, Chem. Phys. Lett. 599 (2014) 133–138.
[15] F. Giberti, A.A. Hassanali, The excess proton at the air-water interface: The role of instantaneous liquid interfaces, J. Chem. Phys. 146 (2017) 244703.
[16] C.A. Daly Jr., L.M. Streacker, Y. Sun, S.R. Pattenaude, A.A. Hassanali, P.B. Petersen, S.A. Corcelli, D. Ben-Amotz, Decomposition of the experimental raman and infrared spectra of acidic water into proton, special pair, and counterion contributions, J. Phys. Chem. Lett. 8 (2017) 5246–5252.
[17] W.H. Robertson, E.G. Diken, E.A. Price, J.W. Shin, M.A. Johnson, Spectroscopic determination of the OH^- solvation shell in the $OH^-(H_2O)_n$ clusters, Science 299 (2003) 1367–1372.
[18] E.F. Aziz, N. Ottosson, M. Faubel, I.V. Hertel, B. Winter, Interaction between liquid water and hydroxide revealed by core-hole de-excitation, Nature 455 (2008) 89–91.
[19] Y. Crespo, A. Hassanali, Unveiling the Janus-like properties of OH, J. Phys. Chem. Lett. 6 (2015) 272–278.
[20] Y. Crespo, A. Hassanali, Characterizing the local solvation environment of OH- in water clusters with AIMD, J. Chem. Phys. 144 (2016) 074304.
[21] S. Heinbuch, F. Dong, J.J. Rocca, E.R. Bernstein, Single photon ionization of van der Waals clusters with a soft x-ray laser: $(CO_2)_n$ and $(CO_2)_n(H_2O)_m$, J. Chem. Phys. 125 (2006) 154316.
[22] T. Habteyes, L. Velarde, A. Sanov, Photodissociation of CO_2^- in water clusters via Renner-Teller and conical interactions, J. Chem. Phys. 126 (2007) 154301.
[23] N. Stafford, Future crops – the other greenhouse effect, Nature 448 (2007) 526–528.
[24] S. Balasubramanian, A. Kohlmeyer, M.L. Klein, Ab initio molecular dynamics study of supercritical carbon dioxide including dispersion corrections, J. Chem. Phys. 131 (2009) 144506.
[25] K.S. Thanthiriwatte, J.R. Duke, V.E. Jackson, A.R. Felmy, D.A. Dixon, High-level ab initio predictions of the energetics of $(CO_2)_m(H_2O)_n$ (n = 1–3, m = 1–12) clusters, J. Phys. Chem. A 116 (2012) 9718–9729.
[26] K.H. Lemke, T.M. Seward, Thermodynamic properties of carbon dioxide clusters by M06–2X and dispersion-corrected B2PLYP-D theory, Chem. Phys. Lett. 573 (2013) 19–23.
[27] Y. Danten, T. Tassaing, M. Besnard, Ab initio investigation of vibrational spectra of water-$(CO_2)_n$ complexes (n = 1, 2), J. Phys. Chem. A 109 (2005) 3250–3256.
[28] A. Muraoka, Y. Inokuchi, N. Nishi, T. Nagata, Structures of $(CO_2)_n(H_2O)_m^-$ (n = 1–4, m = 1,2) cluster anions. I. Infrared photodissociation spectroscopy, J. Chem. Phys. 122 (2005) 094303.
[29] A. Muraoka, Y. Inokuchi, N.I. Hammer, J.-W. Shin, M.A. Johnson, T. Nagata, Structural evolution of the $(CO_2)_n(H_2O)^-$ cluster anions: quantifying the effect of hydration on the excess charge accommodation motif, J. Phys. Chem. A 113 (2009) 8942–8948.
[30] Y. Inokuchi, Y. Kobayashi, A. Muraoka, T. Nagata, T. Ebata, Structures of water-CO_2 and methanol-CO_2 cluster ions: $H_2O(CO_2)_n^+$ and $CH_3OH(CO_2)_n^+$ (n = 1–7), J. Chem. Phys. 130 (2009) 154304.
[31] J. Cuny, A.A. Hassanali, Ab initio molecular dynamics study of the mechanism of proton recombination with a weak base, J. Phys. Chem. B 118 (2014) 13903–13912.
[32] M.J. Frisch et al., Gaussian 09, Gaussian Inc., Wallingford, CT, USA, 2009.
[33] Z. Zhao, X.T. Kong, X. Lei, B.B. Zhang, J.J. Zhao, L. Jiang, Early stage solvation of protonated methanol by carbon dioxide, Chin. J. Chem. Phys. 28 (2015) 501–508.
[34] E.P.L. Hunter, S.G. Lias, Evaluated gas phase basicities and proton affinities of molecules: an update, J. Phys. Chem. Ref. Data 27 (1998) 413–656.
[35] T.D. Vaden, C.J. Weinheimer, J.M. Lisy, Evaporatively cooled $M^+(H_2O)$Ar cluster ions: infrared spectroscopy and internal energy simulations, J. Chem. Phys. 121 (2004) 3102–3107.
[36] R.S. Walters, E.D. Pillai, M.A. Duncan, Solvation dynamics in $Ni^+(H_2O)_n$ clusters probed with infrared spectroscopy, J. Am. Chem. Soc. 127 (2005) 16599–16610.
[37] G.E. Douberly, A.M. Ricks, B.W. Ticknor, M.A. Duncan, Structure of protonated carbon dioxide clusters: infrared photodissociation spectroscopy and ab initio calculations, J. Phys. Chem. A 112 (2008) 950–959.
[38] A.B. Wolk, C.M. Leavitt, E. Garand, M.A. Johnson, Cryogenic ion chemistry and spectroscopy, Acc. Chem. Res. 47 (2014) 202–210.
[39] L. Jiang, T. Wende, R. Bergmann, G. Meijer, K.R. Asmis, Gas-phase vibrational spectroscopy of microhydrated magnesium nitrate ions $[MgNO_3(H_2O)_{1-4}]^+$, J. Am. Chem. Soc. 132 (2010) 7398–7404.
[40] T. Wende, M. Wanko, L. Jiang, G. Meijer, K.R. Asmis, A. Rubio, Spectroscopic characterization of solvent-mediated folding in dicarboxylate dianions, Angew. Chem. Int. Ed. 50 (2011) 3807–3810.
[41] M. Okumura, L.I. Yeh, Y.T. Lee, The vibrational predissociation spectroscopy of hydrogen cluster ions, J. Chem. Phys. 83 (1985) 3705–3706.
[42] E.J. Bieske, O. Dopfer, High-resolution spectroscopy of cluster ions, Chem. Rev. 100 (2000) 3963–3998.
[43] N.R. Walker, R.S. Walters, M.A. Duncan, Frontiers in the infrared spectroscopy of gas phase metal ion complexes, New J. Chem. 29 (2005) 1495–1503.
[44] T.R. Rizzo, J.A. Stearns, O.V. Boyarkin, Spectroscopic studies of cold, gas-phase biomolecular ions, Int. Rev. Phys. Chem. 28 (2009) 481–515.
[45] K.R. Asmis, D.M. Neumark, Vibrational spectroscopy of microhydrated conjugate base anions, Acc. Chem. Res. 45 (2012) 43–52.
[46] L. Jiang, S.-T. Sun, N. Heine, J.-W. Liu, T.I. Yacovitch, T. Wende, Z.-F. Liu, D.M. Neumark, K.R. Asmis, Large amplitude motion in cold monohydrated dihydrogen phosphate anions $H_2PO_4^-(H_2O)$: infrared photodissociation spectroscopy combined with ab initio molecular dynamics simulations, Phys. Chem. Chem. Phys. 16 (2014) 1314–1318.
[47] S.-T. Sun, L. Jiang, J.W. Liu, N. Heine, T.I. Yacovitch, T. Wende, K.R. Asmis, D.M. Neumark, Z.-F. Liu, Microhydrated dihydrogen phosphate clusters probed by gas phase vibrational spectroscopy and first principles calculations, Phys. Chem. Chem. Phys. 17 (2015) 25714–25724.
[48] M.R. Fagiani, H. Knorke, T.K. Esser, N. Heine, C.T. Wolke, S. Gewinner, W. Schoellkopf, M.-P. Gaigeot, R. Spezia, M.A. Johnson, K.R. Asmis, Gas phase vibrational spectroscopy of the protonated water pentamer: the role of isomers and nuclear quantum effects, Phys. Chem. Chem. Phys. 18 (2016) 26743–26754.
[49] H. Wang, N. Agmon, Complete assignment of the infrared spectrum of the gas-phase protonated ammonia dimer, J. Phys. Chem. A 120 (2016) 3117–3135.
[50] D. Marx, M. Parrinello, Ab initio path integral molecular dynamics: basic ideas, J. Chem. Phys. 104 (1996) 4077–4082.

[51] O. Vendrell, M. Brill, F. Gatti, D. Lauvergnat, H.-D. Meyer, Full dimensional (15-dimensional) quantum-dynamical simulation of the protonated water-dimer III: Mixed Jacobi-valence parametrization and benchmark results for the zero point energy, vibrationally excited states, and infrared spectrum, J. Chem. Phys. 130 (2009) 234305.
[52] J.M. Bowman, B.J. Braams, S. Carter, C. Chen, G. Czako, B. Fu, X. Huang, E. Kamarchik, A.R. Sharma, B.C. Shepler, Y. Wang, Z. Xie, Ab-initio-based potential energy surfaces for complex molecules and molecular complexes, J. Phys. Chem. Lett. 1 (2010) 1866–1874.
[53] Y. Wang, J.M. Bowman, IR spectra of the water hexamer: theory, with inclusion of the monomer bend overtone, and experiment are in agreement, J. Phys. Chem. Lett. 4 (2013) 1104–1108.